Tampere University

Manas Bimagambetov

“LITERATURE REVIEW ON GLASS-BASED MATERIALS DEVELOPMENT FOR APPLICATIONS AT 2.7µM”

Faculty of Engineering and
Natural Sciences
Bachelor of Science Thesis
December 2021

ABSTRACT

Manas Bimagambetov: Glass-based materials development for MIR applications at 2.7μm Bachelor of Science Thesis
Tampere University
Bachelor's Programme in Engineering and Natural Sciences
December 2021

The goal of this thesis was to review the work performed worldwide on the development of novel optical glass-based materials for mid-infrared sensing applications. The study focused on tellurite, germanate and phosphate glass and glass-ceramics. The $^4I_{11/2} \rightarrow {}^4I_{13/2}$ transition of Er^{3+} under 980 nm laser excitation corresponding to a 2.7 μm emission was targeted

This thesis describes the applications targeted in the mid-infared region and how glass could be the best support to reach those applications. A review of the materials used for the specific 2.7 μm emission is made: mid-infrared glasses doped with Er^{3+} are interesting when a typical 980 nm laser diode is used for excitation. A literature review on the different techniques used to improve the 2.7 μm emission is also presented.

Keywords: Glass; Glass-ceramic; luminescence; rare-earth ions

The originality of this thesis has been checked using the Turnitin OriginalityCheck service.

PREFACE

This thesis was pulled off under the Bachelor's Programme in Engineering and Natural Sciences at Tampere University. The research was done in the Photonic Glasses research group under the supervision of Dr. Arnaud Lemiere and Prof. Laeticia Petit in the Laboratory of Photonics.

For very first, I would like to thank Professor Laeticia Petit for her supervision and help during the autumn semester. Also, I would like to acknowledge Arnaud Lemiere for his support and help with writing as well as processing the collected data. And I would like to thank all for their help and advice.

Tampere, 6 December 2021

Manas Bimagambetov

CONTENTS

LIST OF FIGURES

LIST OF SYMBOLS AND ABBREVIATIONS

A	Absorption
c	speed of light
E	Energy
T	Temperature
ΔT	Temperature difference
°C	Celsius Degrees (0 °C = 273.15 K)
g	Gram (1 g = 10^{-3} kg)
μm	Micrometer (1 μ = 10^{-6} m)
nm	Nanometer (1 nm = 10^{-9} m)
a.u.	Arbitrary Unit
LD	Laser diode
GL and GY	germanate glasses modified by La_2O_3 and Y_2O_3 respectively
HT	Heat-treatment
IR	Infrared
mol%	mole present
NP	Nanoparticle
RE	Rare-earth
T_g	Glass transition temperature
T_m	Glass melting temperature
T_p	Crystallization peak temperature
T_x	Crystallization onset temperature
Ag	Silver
$NaYF_4$	Sodium Yttrium Fluoride
$LiYF_4$	Fluoride Laser Crystals
AgCl	Silver chloride
Bi_2O_3	Bismuth(III) oxide
Er_2O_3	Erbium(III) oxide
Er^{3+}	Erbium ion

1 INTRODUCTION

The demonstration of the laser effect nearly 60 years ago marked the beginning of the era of optics and photonics [3, 4]. Since the beginning of the 21st century, photonic technologies have become more and more ubiquitous in everyday life and in a wide variety of sectors. Today, the influence of photonics in modern technology is still growing and an even greater effect in the next decades is foreseeable. Optics and photonics have undergone remarkable technological developments over the past decades and have established themselves as key enabling technologies for a wide variety of industries. The magnitude of the impact of photonics in technology can be measured by the number of innovations developed using photonics. In 2011, 12 of the top 50 innovations listed by Time Magazine used optics and photonics as a core technology [5].

Coherent mid-infrared (MIR) light sources have recently gained popularity in research and development because of rotational and vibrational absorption peaks of molecular gases (such as pollutants and greenhouse gases) absorbing in the MIR region. At 2.4 μm, 2.7 μm, 2.8 μm 3.3 μm and 3.5μm, respectively, CO, H_2O, CO_2, CH_4 and NO_2 show high absorption peaks. MIR light sources could be then used for sensing molecules and that technology might be used to detect and monitor air pollution from industry and airplanes, as well as the detection of drugs and explosives for security screening. Water absorbs strongly at 2.7 μm, making MIR Light sources also useful in sectors such as medicine, remote sensing, and environmental monitoring [6, 7].

Er^{3+} doped materials are becoming a research hotspot because of the emission of Er^{3+} ions at 2.7 μm, and the convenient pumping wavelength; indeed the absorption bands of Er^{3+}-ions correspond to the widely accessible and low-priced 808 nm or 980 nm LD [8]. To achieve emission at 2.7 μm, it is necessary to consider both the active ions and the host material. Selecting a suitable host material is crucial because of the emission wavelength. However, because the Er^{3+} transition ${}^4I_{11/2} \rightarrow {}^4I_{13/2}$ has low energy, multi-photon relaxation may dominate infrared emissions when the glass contains high phonon energy [9, 10]. Germanates and tellurite glasses, for example, have maximal phonon energies of roughly 900 cm^{-1} and 700 cm^{-1}, appropriately making them low-phonon-energy glasses with excellent MIR transmission. They are much more acceptable as hosts for MIR emission than silicate glasses with maximal phonon energy of around 1100 cm^{-1} [11].

Beyond the introduction, the thesis moves on to Chapter 2, which covers the fundamentals of MIR region and glass theory and processing. A specific focus is then made on the 2.7 μm emission in Chapter 3. Finally, Chapter 4 develops the recent findings on the enhancement of the 2.7 μm emission supported by research papers.

2. BACKGROUND

2.1 MIR spectrum and its applications

2.2.1 Targeted applications in MIR region

Mid-infrared region is the region between 1 and 20 μm and has been targeted for a variety of applications such as gas detection, chemical analysis or medical diagnosis [12]. Many greenhouse gases or other polluting molecules, as seen in Figure 1, have intense absorptions (strong characteristic vibrational and rotational transitions) between 2 and 5 μm (CH_4, H_2O, OH, CO_2, SO_2, N_2O, CO, O_3). The intensities of these chemical species' absorptions are shown according to their wavelength. MIR spectroscopy is also an effective chemical analysis technique for detecting biomedically important constituents such as DNA/RNA, proteins, carbohydrates, lipids, as well as diseases that may cause changes in the chemical signature of a biological systems. [9]

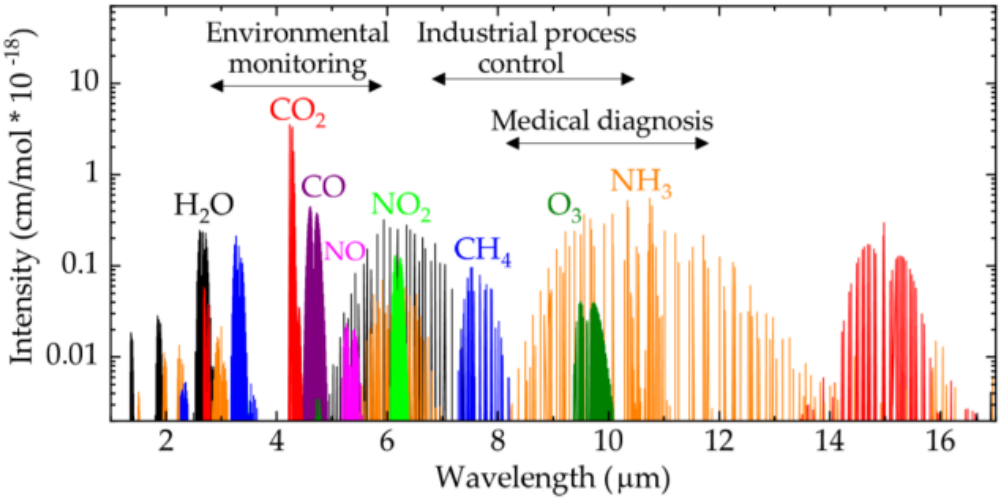

Figure 1. Mid-infrared absorption spectra of selected molecules with their relative intensities. H_2O: water; CO_2: carbon dioxide; CO: carbon monoxide; NO: nitric oxide; NO_2; nitrogen dioxide; CH_4: methane; O_3: oxygen; NH_3: ammonia [48]

MIR region is then critical to reach for detecting and processing a wide range of molecules. Recent advances in spectra acquisition techniques and advanced materials fabrication has made of IR spectroscopy a new powerful sensing instrument: MIR spectroscopy wavelength in range 2-20 μm, today offers molecular knowledge with trace to ultra-trace sensitivity, rapid data acquisition speeds, and high spectral resolution, making it suitable for challenging applications such as bio analytics and routine processing [48].

2.2.2 Materials for MIR applications

To satisfy the expanding demands of these applications, there has recently been a rise in interest in innovative Mid-infrared optical materials and associated device implementations. Among the compositions, the most promising glass composition for the manufacturing of Erbium-doped is GC-materials and polymers. Typically doped with RE ions, GCs integrate glass features (great compositional and geometrical flexibility) with several of the features of RE-doped single crystals (higher absorption, emission and lifetimes). Low-phonon-energy crystals and glasses with rare-earth doping are promising lasing media in the 2-3 μm range. Low phonon energy hosts, such as germanate, chalcogenide, tellurite, or fluoride glasses, favor the RE ions' radiative transitions and enable specific radiative transitions at wavelengths that would otherwise be quenched in silica or phosphate glasses (for example, the transition $^4I_{11/2} \rightarrow {}^4I_{13/2}$ results in emission at 2.7 μm). Low phonon energy hosts, on the other hand, do not have the same physical and chemical characteristics as silicate or phosphate glasses.

2.2 Sensing

2.2.1 Principle of sensing

Raman and infrared spectroscopies have been used to explore the crystallization process as well as the structural, optical, and luminescence features of Er^{3+}-doped phosphate glass-ceramics.

ATR is one of the most often used techniques in Fourier Transform Infrared Spectroscopy for analyzing materials (FTIR). The FTIR approach is popular because it enables the study of solid and liquid samples in their purest form, hence facilitating the evaluation of nearly any material. ATR spectroscopy is a method for determining the structure and composition of a material. A beam of light is focused on the sample in spectroscopy. The powerful way length for this communication relies upon a few boundaries and is regularly a small amount of a frequency. In view of the little light entrance profundity, the ATR method is great for profoundly absorbing samples and for surfaces and flimsy film estimations. By and large, the ATR spectra are like customary transmission; notwithstanding, for thick examples when spectra are recorded at points more prominent than the basic one, the frequency reliance is noticed [55].

The sample is in contact with an FTIR crystal. Infrared radiation penetrates through the crystal and reacts with the sample on the NPBO crystal's surface. Due of the two materials dissimilar refractive indices, complete internal reflection occurs. This reflection results in the formation of an "evanescent wave" that propagates deep inside the sample. Depending on the sample's composition, a tiny amount of infrared light is absorbed during the interaction of the attenuation wave with the sample, resulting in a slightly attenuated total reflection.

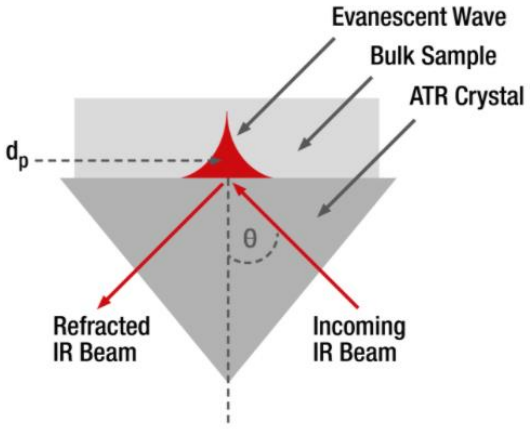

Figure 2. Evanescent wave resulting from total internal reflection

The penetration depth indicates how deeply the evanescent wave penetrates the sample. If analyte molecules are present on the waveguide surface or within d_p, they may interact with the evanescent field generated at the waveguide sample interface, resulting in attenuation of the propagating wave at frequencies in resonance with the corresponding molecular vibrations and/or rotations [53].

$$d_p = \frac{\lambda}{2\pi n_1 \sqrt{sin^2\theta - \frac{n_1}{n_2}}},$$

where λ is wavelength of incident light in vacuum, d_p is a penetration depth, n_1 is a refractive index of ATR crystal (dense medium) and n_2 is a refractive index of sample (rare medium).

Absorption inside the evanescent field follows a pseudo Beer Lambert relationship, allowing for measurement of the chemical signatures gained [52]. Lambert and Beer's Laws associate the radiant power of a beam of electromagnetic radiation, most commonly ordinary light, to the length of the beam's passage in an absorbing medium and the concentration of the absorbing species, respectively.

$$\log\left(\frac{I_0}{I}\right) = A = (\boldsymbol{\epsilon CL})\boldsymbol{r}$$

where I and I_0 are irradiance of light measured by detector and initial irradiance, respectively

It asserts that the absorbance of a material sample is directly related to its thickness (path length) and attenuating species concentrations. Pierre Bouguer identified the relationship between absorbance and material thickness before 1729. The Beer-Lambert Law never fails [53] when monochromatic light is utilized and [54] when the concentration component in the law is the concentration of the absorbing species. Clearly, the rule will not hold in general if another species' concentration is added as c, even if the absorbing species is in equilibrium with the other species [53]. Chemical analysis measures are the most common place where the legislation is used in practice. Attenuation of solar radiation by aerosols - suspensions of

small solid particles or liquid droplets is another real-world phenomenon that may be explained by Beer-Lambert equation.

Due to the fact that the number of reflections is inversely proportional to the thickness of the waveguides, reducing the thickness of the waveguide layer directly affects the dielectric constant at the interface, which is influenced by the materials, cross-sectional dimensions, and thickness of the waveguide as shown in Figure 3.

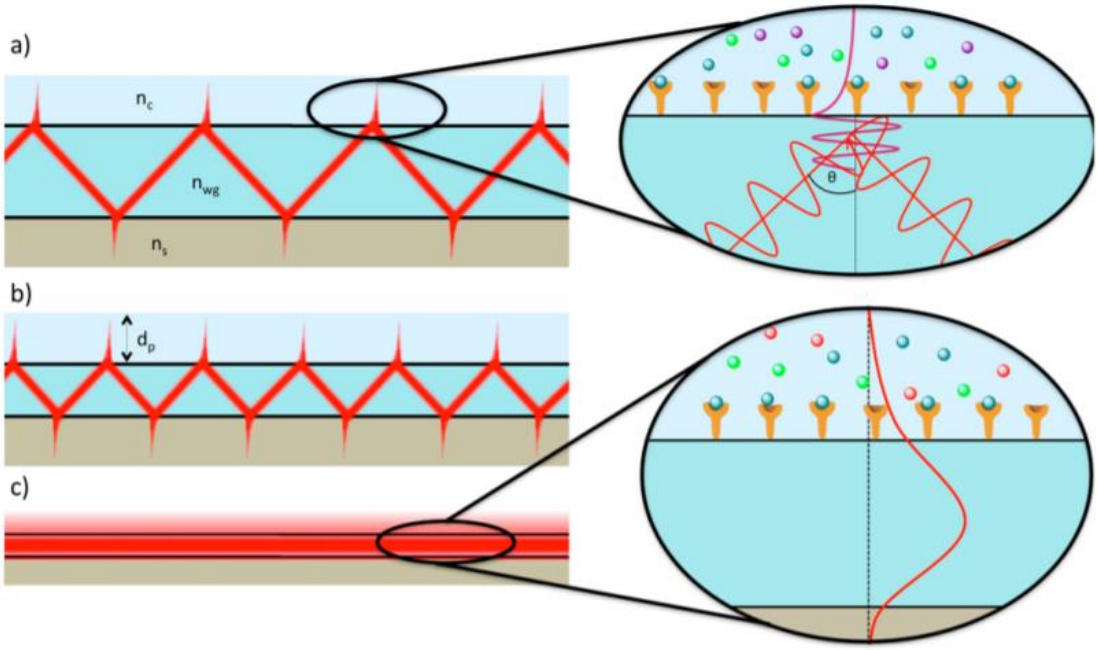

Figure 3.Planar waveguide with sample, waveguiding, and substrate layers with nwg > ns, n[51]

2.2.2 Waveguide fabrication

The literature gives many examples of the use of optical fibers and thin films for MIR applications.

2.2.2.1 Film deposition

Thin film is the name given for sub-μm thick layer of glass deposited on a substrate. Thin film deposition technology allows us to fabricate planar waveguides or channel waveguides which provide different light propagation properties. There are many techniques to use to deposit films.

For example, from the sol-gel chemistry technique, two simple ways of thin film fabrication are possible: **spin-coating and dip-coating**. In the sol-gel chemistry technique, the inorganic polymerisation processes are used to create an oxide network from molecular precursors. The sol-gel process has various advantages such as it does not require power-consuming, expensive equipment is much more economical and it is environmentally friendly. This technique also allows to obtain materials of complex chemical composition

and structure and coatings of remarkable purity with the required properties. In this chemical procedure, the symbol " sol " (colloidal solution) gradually evolves to form a gel like two-phase system containing both the liquid phase and the solid phase. Removing the remaining liquid (solvent) stage requires a drying process usually accompanied by a significant amount of shrinkage and densification. Heat treatment or roasting is often necessary to promote further polycondensation and improve mechanical and structural properties stability through final sintering, densification, and grain growth. One clear advantage of using this methodology over more traditional processing methods is that densification is often achieved at much lower temperatures. The sol-gel approach is a low cost and low-temperature method that allows precise control of the product's chemical composition. Even small amounts of alloying agents such as organic dyes and rare earth elements can be introduced into the “sol” and ultimately evenly dispersed in the final product. It can be used in the processing and production of ceramics as a material for investment casting or the production of thin film metal oxide films for various purposes. Materials based on sol-gel are used in multiple applications in optics, electronics, energy, space, (bio) sensors, medicine.
The sol precursor can be applied to a substrate with film formation (e.g. by dip coating or rotating coating), cast into a suitable container of the desired shape (e.g. to produce monolithic ceramics, glass, fibres, membranes, aerogels), or used for powder synthesis (e.g. microspheres, nanospheres).

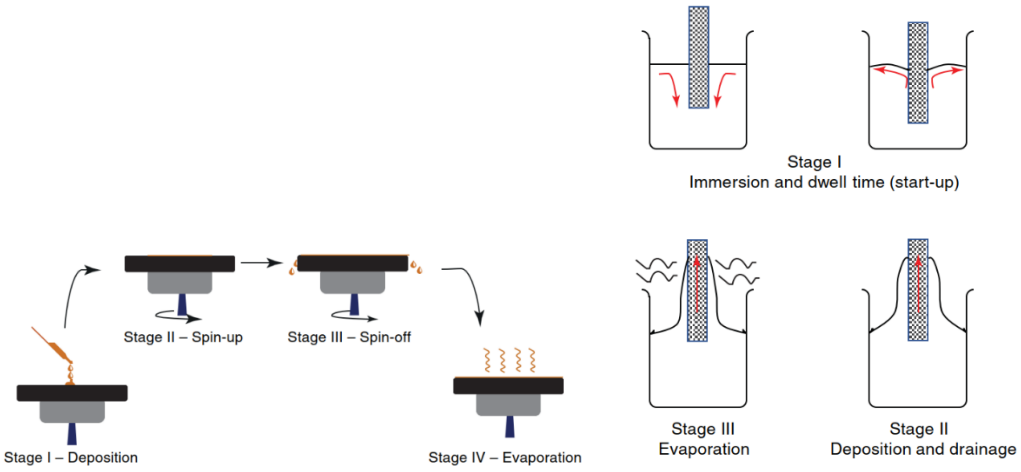

Figure 4: spin-coating process (left) and Dip-coating process (right) (L. E. Scriven, 2011)

Films can also be obtained based on vacuum processes. These processes are typically categorized based on physical vapor deposition (PVD) and chemical vapor deposition (CVD).[49]

- **PVD** is a general concept for quantifying processes for film deposition. The material goes from a condensed phase to a vapor phase and then back to a thin film condensed phase.in a partial vacuum setting. Coatings are highly scratch- and corrosion-resistant. Electron-beam evaporation deposition, pulsing laser deposition, molecular beam epitaxy, and sputtering are all examples of PVD techniques, as are other types of deposition processes.[38] PVD method provides high quality material but is expensive and may need a substantial quantity of material.

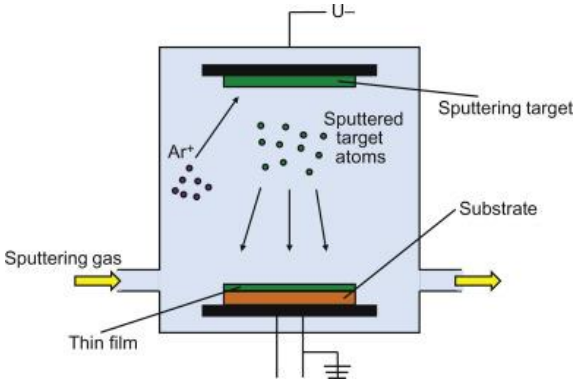

Figure 5: Simplified model of physical vapor deposition (PVD)

- **CVD** is commonly used around the world because it is possible to manufacture sufficient-quality thin films at a lower cost. A method of producing high-purity solid materials. The process is often used in the semiconductor industry to create thin films. Typically in the CVD process, a substrate is placed in a vapor of one or more substances that react and decompose to produce the desired substance on the surface of the substrate. The gaseous reaction product is often formed, which is carried out of the chamber with the gas flow [49]. The main feature of CVD technological methods is the flow of chemical reactions between the gas constituents of the working atmosphere, which leads to the formation of thin solid layers on the surface of the base material. This is possible under strictly defined thermodynamic conditions, primarily at high temperatures and corresponding pressures.

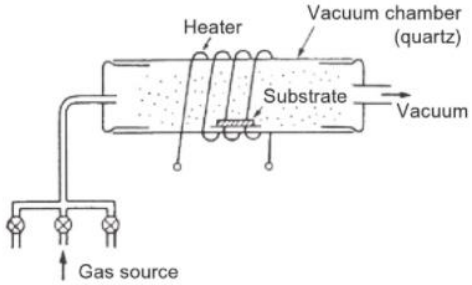

Figure 6: Chemical vapor depositions (CVD)

2.2.2.3. Fiber drawing process

The main advantage of optical fiber is the flexible property of this material. Optical fiber is mainly used for telecommunications (silica optical fibers). The commercialized optical fiber is coaxial in structure, with a core to guide light and a clad, surrounded by acrylate coating.

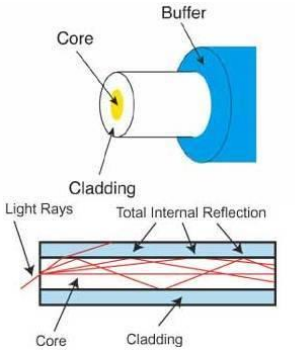

Figure 7: Core-clad fiber

-The melt quenching method is well adapted to the fiber drawing process because glass preforms can be easily realized in a preheated mold. The melting process to process a glass rod can be explained by the schematic below.

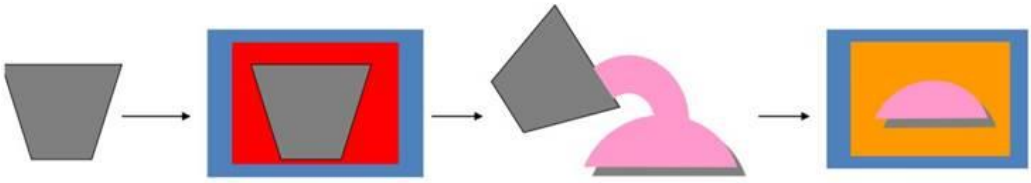

Figure 8: Representation of the different steps of the melt-quenching method : 1- Mixture of raw materials, 2- melting at high temperature, 3- Quenching

The Figure 8 displays the elements that make up a drawing tower. A furnace generates heat at a specific position of the glass rod. The glass rod is softened during the furnace heating ramp until fall because of gravity as soon as the viscosity of the rod decreased enough. A glass rod composed of a top part, a fiber part and a lower part is then obtained as visible on the left part of the Fig 8. Inert gas is used to avoid atmospheric pollution in the glass. and unfavourable oxidizing environment inside the heating zone. The translation system allows to feed the heating position with adjusting the position of the glass preform. The diameter and tension measuring tools enable the fiber diameter and pulling force to be evaluated. A UV lamp is available if the fiber needs to be coated with a polymer layer and finally a drum is available to store the newly processed optical fiber. Throughout the fiber drawing process, this flow is maintained.

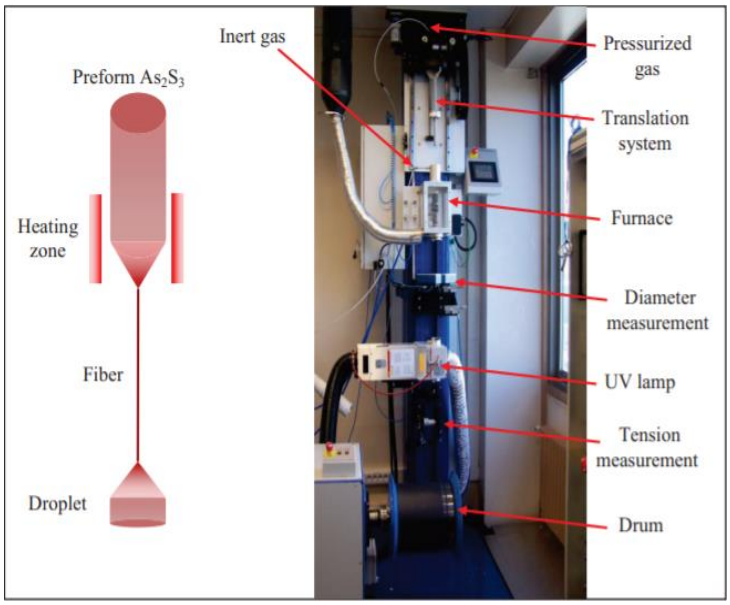

Figure 9: Glass rod geometrical evolution during drawing process (left) and drawing tower (right) [39]

3. GLASS-BASED MATERIALS FOR MIR EMISSION

3.1. Glass-based materials

3.1.1 Glass definition and glass formation theory

Although glass has all the mechanical properties of a solid, it is a material presenting the properties of a “frozen liquid”. Glass is an amorphous (non-crystalline) solid, meaning that no long range order is visible in its composition: atoms are almost randomly arranged in the glass matrix. Only a short-range order is visible in glass, meaning that molecules keep present as molecules (SiO_2 stays SiO_2 in the glass, for example). The distinction between a crystal, a liquid, and a glass is seen in Figure 9.

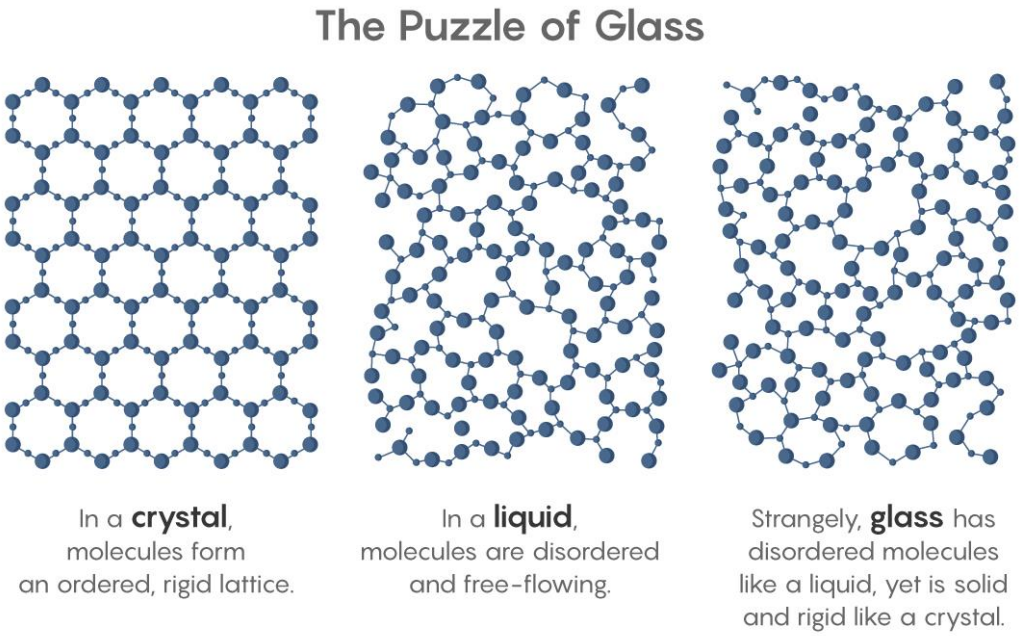

Figure 10: Two-dimensional schematic of a SiO2 atomic structure in a (left) crystalline material, (center) liquid and (right) amorphous material [11]

We can see in figure that glass has the atomic structure of a liquid but still has the mechanical properties of a solid. Glass, unlike crystals, lacks a long-range periodic structure and lattice since bond orientations differ greatly. That atomic structure of glass induces its thermal properties. They would not have a clear melting point; rather, their viscosity drops dramatically at a specific temperature (glass transition temperature). The figure 11 shows how a crystal and a glass cool down at low temperature.

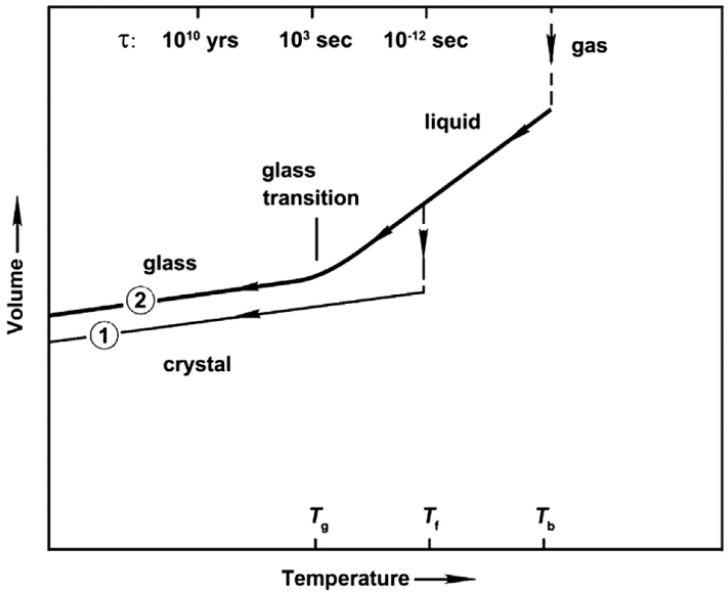

Figure 11: Schematic plot illustrating the change in specific volume of a glass with temperature [12]

We can see in Figure 10 two paths for the solidification process: number 1 is related to the crystal formation and number 2 is related to the glass formation. When a liquid is cooled down, it usually follows path number 1 and exhibits a temperature where the crystal formation occurs (T_f). A volume reduction is linked to the atomic structure arrangement and the newly formed crystal continue to cool down. Glass exhibits the presence of a distinct glass transition temperature (T_g). If the liquid batch is cooled quickly enough to solidify it, the atomic structure will not be able to arrange itself, and the liquid will become solid without structural arrangement (path 2). We then obtain a supercooled liquid (highly viscous liquid), which exhibits a T_g. At T_g, the viscosity of the liquid reaches the value of 10^{13} poises. Below that temperature, we have a glass, which is an amorphous solid.

One of the main advantages of glass is that there is theoretically an infinity of glass materials due to the ability to change the glass composition. Thanks to this, we can pick a glass family and adapt the composition depending on the properties we need (refractive index, optical transmission, glass transition temperature).
In addition to the glass matrix, we can add a variety of dopants elements, including rare-earth (RE) ions, to modify or add some properties to the glass. Those elements will be inserted into the glass structure and modify the properties of the glass. Rare-earth dopant, specifically, will allow to give new optical properties to a glass such as luminescence properties. Among other things, these properties make glasses excellent hosts for optical and photonic applications.

3.1.2 Crystals in glass

Even in daily life, glass-ceramics are used in various applications, including cookware, electric stovetops, building materials, telescope mirrors, liquid crystal displays, solar cells, and photonic devices [40]. Due to the vast amount of interest in this nanostructured material, researchers have been focusing their efforts on characterizing the crystallization mechanisms

of numerous glass families, including silicate [4, 5], tellurite [6], and chalcogenide glasses [7], to name a few. A glass-ceramic is often not entirely crystalline; the microstructure is typically 50–95 % crystalline, the balance being residual glass. During heat treatment, one or more crystalline phases may emerge, and since their composition is generally distinct from the precursor (parent) glass, the leftover glass's composition is likewise different from the parent glass. Despite the fact that glass-ceramics are a transitional material between glass and crystal, there is the possibility of obtaining the best properties of each of these two materials, as well as the simplest method of fabricating a glass with crystal-like spectroscopic properties due to the ability of some crystalline phases to selectively partition optically active ions into the crystal phase[41, 42]. The highest vibrational energy of the crystal phase may also be lower. This minimizes the potential of non-radiative relaxations from the exciting stages of the RE, hence improving the radiative decay paths [41].

A crystalline environment may alter the luminescence qualities in addition to modifying the composition surrounding the Er^{3+} ions. The crystals may precipitate as a result of a thermal treatment of the glass. Crystals may be put to the glass as well. RE ions are homogeneously distributed throughout the glass matrix in RE-doped glasses, however RE ions may be integrated in a crystalline structure isolated from the glass matrix in RE-doped GCs and particles containing glasses.

3.1.3 Glass-ceramic method

A glass-ceramic is a glass containing crystalline phases in its structure. Those crystals are produced by heat treatment process [43]. During heat treatment, one or more crystalline phases may emerge, and their composition is generally distinct from the precursor glass. Even though glass-ceramics are a transitional material between glass and crystal, there is the possibility of obtaining the best properties of each of these two materials [41, 42]. The highest vibrational energy of the crystal phase may also be lower. This minimizes the potential of non-radiative relaxations from the exciting stages of the RE, hence improving the radiative decay paths [41]. It is critical to highlight that specific glass compositions are appropriate as precursors for glass-ceramics. Some glasses, such as conventional window glass, are too stable and difficult to crystallize, while others crystallize too quickly and uncontrollably, resulting in undesired microstructures.

Glass-ceramics, when doped with RE ions, combine glass qualities with specific benefits of RE-doped single crystals (increased absorption, emission, and lifetimes). Furthermore, these materials have outstanding mechanical qualities such as compressive and bending strength [14] and outstanding thermal endurance. Numerous families of Glass-ceramics have been examined in terms of crystallization mechanisms, including tellurite [15], chalcogenide [14], silicate [17], and phosphate glasses [14]. It provides information on how the crystallization process is affected by temperature.

Glass-ceramics are made by heat-treatment. The crystallization of GCs is divided into two stages as shown in Fig.12: the first is the nucleation of tiny nuclei, and the second one is the development of those nuclei into crystals (growth stage). It is necessary to identify the best temperatures of these two stages for each glass composition [42].

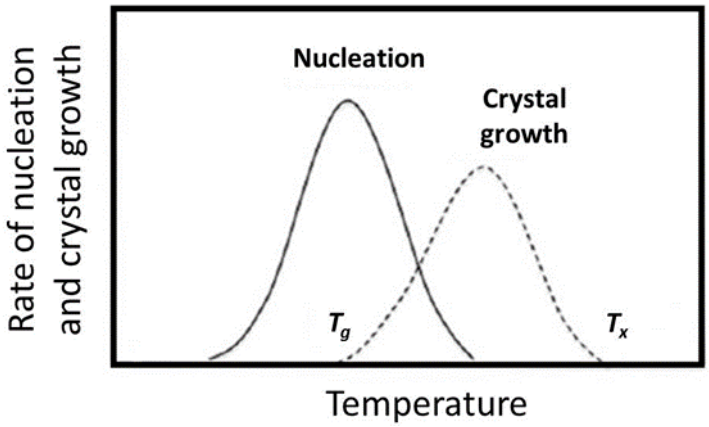

Figure 12: The nucleation and crystal growth rates as a function of temperature. The figure has been changed from [41].

Gibbs's free energy, activation energy, and other factors influence the lowest energy needed to produce nuclei with a critical radius. Instable nuclei smaller than the crucial radius tend to dissolve back into the matrix, but crystal formation may be stimulated by more prominent nuclei than the critical radius. The critical radius may be as small as a few tenths of a nanometer after the thermodynamic and kinetic barriers have been overcome. Furthermore, by adding more atoms or molecules to the previously created nucleus, crystallization of the glass might be achieved.

While glass is in a thermodynamically stable condition, it turns into an ordered structure with a decreased free energy during crystallization. The crystalline phase has lower energy than the glass phase, hence the volume energy drops when the glass phase transitions into the crystalline phase. A new interface, on the other hand, requires time and resources. The figure 13 depicts the energy interaction because of the nucleus radius.

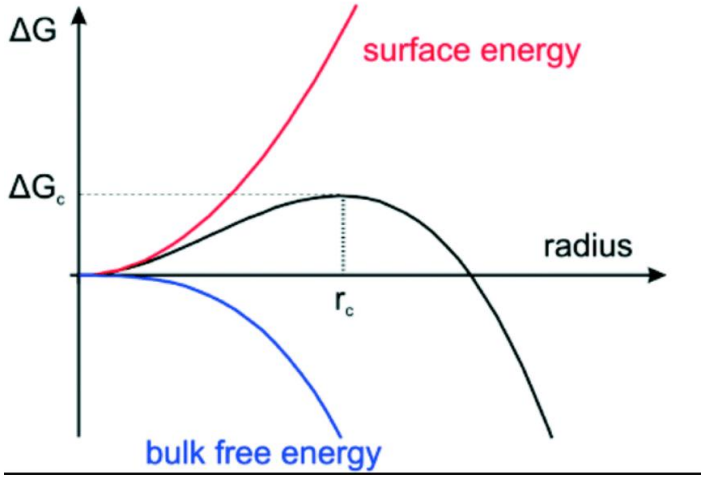

Figure 13: The interaction of the volume energy and the interfacial energy as a function of the nucleus radius [28]

3.1.4 Direct doping process

Direct doping method (DDM) consists in adding Er^{3+}-doped particles in the glass melt before the quenching. it is then possible to have a glass with specific particles inside. The DDM allows for incorporating particles with precise compositions and dopants into the glass. To guarantee particle survivability inside the glass during preparation, the particles must be thermally stable at the doping temperature. As mentioned in [28], the first step is to find a glass composition whose doping temperature is lower than the particle's upper limit. The second stage is to identify two parameters for creating glasses with homogenous particle dispersion: the doping temperature and the dwell time before casting the glasses [28].

The benefits of both glasses (composition and geometrical flexibility) and crystals (higher absorption, emission, and lifetimes) are thus combined [44]. It has the advantage that the local environment of the RE ions is regulated by the particle crystal matrix independent of the glass composition [45]. Zhao [46] in own research used the DDM to improve the spectroscopic properties of nanoparticles-containing tellurite glasses and demonstrated that optical fibers with low losses and up-conversion emission can be obtained using this technique

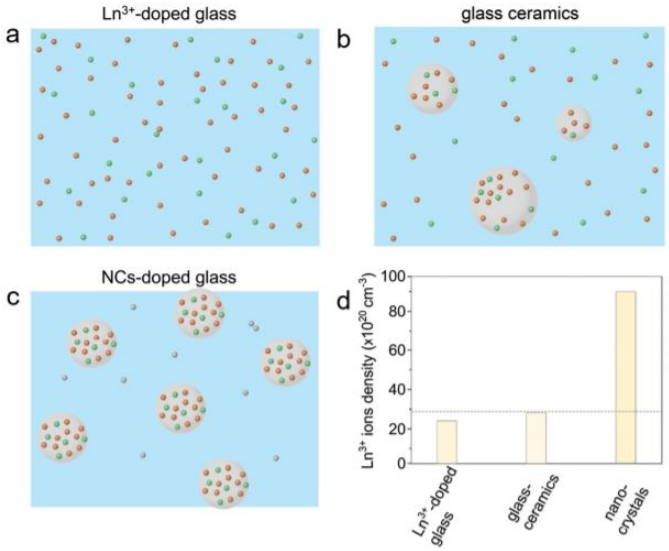

Figure 14: a-c) Theoretical phase results from different fabricating methods and d) the comparison [24].

Figure 14-c depicts the potential outcome of particle doping by direct injection of a chemical compound. Because of the perfect control over the properties of the nanocrystals, it is predicted that the pre-synthesized particles with RE will result in considerable improvements in the final glasses. According to the comparison shown in Figure 14-d, the direct doping approach significantly outperforms the other fabrication methods in terms of RE ion concentration. As previously stated, Zhao et al. have successfully employed the approach to dope telluride glasses with $LiYF_4$ nanoparticles, resulting in some rather remarkable outcomes for their efforts. Despite this, the scientists found a 30-60% loss of nanoparticles in the glass, showing much space for improvement in this area [46].

3.2 LASING GLASSES

3.2.1 Rare-earth ions

The rare-earth ion up-conversion process is amongst the highly effective methods for converting low-energy photons to high-energy photons. It is indeed a photochemical approach in which low-energy photons are transformed into high-energy photons in a supramolecular gel. It required the use of visible light as well as chromophore donor and receiver molecules. As of late, the ideas of spending transformation of the RE particles was stretched out to nanomaterials, albeit customarily it has been broadly read up for mass or fiber-like calculation for applications in high-power laser frameworks and media transmission intensifiers as well as radiance phosphors, secure printing or progressed bioimaging tests[57]

Throughout the long term numerous up-transformation components have been perceived and depicted in the writing, including energy move up-change (ETU), where nonradiative energy move assumes a predominant part, energized state retention up-transformation (ESAU), regularly called consecutive assimilation of two photons, lastly photon torrential slide up-change (PAU), being a particular blend of the ETU and ESAU[56]

In the case of sensitized luminescence, these dopants are further subdivided into sensitizers and activators, where one dopant ion emits photons from its high energetic state because of energy transfer from another dopant ion [57]. Moreover, the doping technique entails presenting a low convergence of particles (for example, dopants) into an inorganic glasslike grid to obtain doped materials, which is widely used to make iridescent materials with high discharge. The dopant ion that emits emission is referred to as an activator, while the ion that contributes energy to the activator is referred to as a sensitizer. Most RE activator ions have limited absorption cross-sections, resulting in poor pump efficiency. As a result, a sensitizer ion with a high absorption cross-section is typically utilized as an energy donor to the activator ion to improve pump efficiency.

3.2.2. Er^{3+} doped glasses

Er^{3+} ion is an ideal luminescent centre for 2.7 μm emission. Figure 15 shows the Er^{3+}-ions energy level diagram.

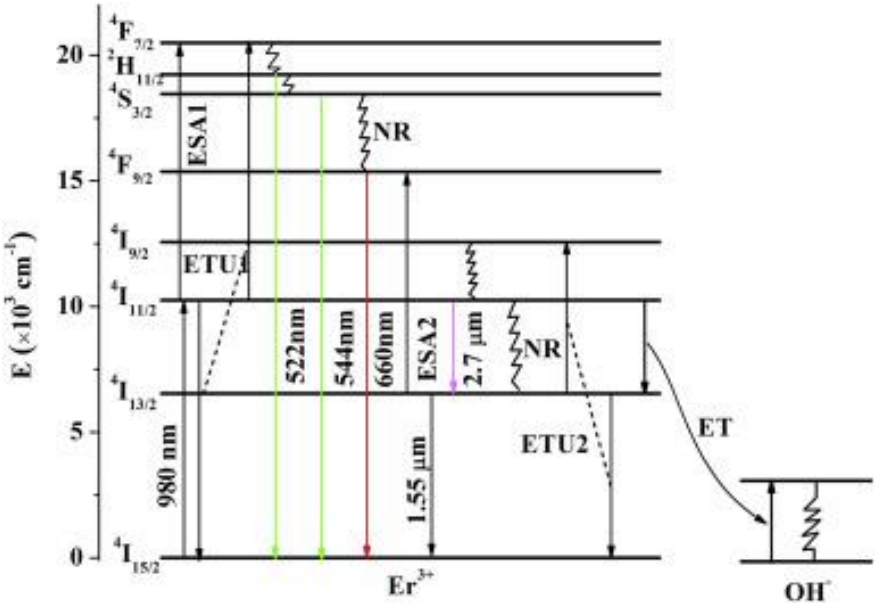

Figure 15: Schematic energy level diagram of Er^{3+}. [37]

It has an emission at 1,5 µm due to the energy level transition $^4I_{13/2} \rightarrow {}^4I_{15/2}$ but also at 2.7 µm because of the $^4I_{11/2} \rightarrow {}^4I_{13/2}$ transition, The Er^{3+}-ions ground state level $^4I_{15/2}$ is excited to the $^4I_{11/2}$state under the 980 nm pumping through the ground state absorption (GSA) process when irradiated at 980 nm. A radiative relaxation can occur leading to a transition o from $^4I_{11/2}$to $^4I_{13/2}$ (2.7 µm emission). Moreover, at the level of $^4I_{13/2}$ Er^{3+}-ions can decay to ground level with emission at 1.55 microns. The energy transfer process (ETU1) is based on excited state absorption (ESA1: $^4I_{11/2} \rightarrow {}^4F_{7/2}$). In $^4F_{7/2}$state, non-radiative relaxation occurs, leading to the population of $^4I_{11/2}$, $^4S_{3/2}$and $^4F_{9/2}$levels, according to the non-radiative relaxation processes (NR). Therefore, $^4I_{11/2} \rightarrow {}^4I_{15/2}$, $^4S_{3/2} \rightarrow {}^4I_{15/2}$ and $^4F_{9/2} \rightarrow {}^4I_{15/2}$ transitions lead to the emissions of 522 nm, 544 nm and 660 nm. ETU2 ($^4I_{13/2} \rightarrow {}^4I_{15/2}$leading to the excitation of the excited state $^4I_{9/2}$) may be beneficial for emissions at 2.7 µm. [37]

3.3 Glass systems for MIR application

To design more effective optical systems, it is necessary to consider the host material in addition to the active ions. Thus, it is critical to search for appropriate host materials for mid-infrared lasers operating at this wavelength.

Tellurite [4], bismuth [9], germanate [11], fluoride [14], and fluorophosphate glasses have all been investigated widely by scientists. According to the low thermal shock resistance, the fluoride glass fiber laser has a lower damage threshold but still exhibits poor mechanical qualities. Furthermore, fluoride and chalcogenide glasses have a low resistance to moisture, are complex to mass manufacture, and are sensitive to humidity. Germanate glass is more thermally stable and mechanically stronger than fluoride, chalcogenide, fluorophosphate, and tellurite glasses due to the greater ionic interaction between Ge^{4+} and O_2 ions [18], [19]. Due to its high mid-infrared transmission (up to 6 µm) [20], relative thermal stability, strong mechanical properties, and great chemical durability when compared to other glasses, germanate

glass has been recommended as an attractive material for optical applications. Additionally, germanate glass has low maximum phonon energy (800–900 cm1), which benefits the likelihood of radiative transitions and the associated mid-infrared emission [21].

Glass	Maximum phonon energy (cm^{-1})
Borate	1400
Silicate	1100
Phosphate	1200
Germanate	900
Tellurite	700
Fluorozirconate	500
Chalcogenide	350

Table 1 maximum phonon energy of few glasses

Germanate glasses are important because they have a lower phonon energy than other type of glasses developed in Er^{3+} at 2.7 μm emissions. Furthermore, high thermal conductivity, chemical resistance, mechanical strength, and transparency which represents transmission range of different glasses in 3-5 μm in the mid-infrared range are just a few of the benefits than other glasses have. Additionally, germanate glasses are well-known for their chemical resistance and remarkable mid-infrared transparency [22]. Erbium emission at 2.7 μm has been seen in a variety of germanate glasses, including fluorotellurite - germanate [20], barium gallo-germanate [21] [22], and glass-ceramics based on germanate [23].

4. ENHANCEMENT OF THE 2.7 µM EMISSION

4.1 Change in glass composition

Over the past decades, research papers have studied phosphate- [13], silicate- [14], tellurite- [18], germanate [32], and fluoride [15] based glasses, as well as glass ceramics [21], to reach the 2.7 µm emission.

Several publications have been published on the 2.7 µm emission from tellurite and bismuthate glass nanocomposites (BGN) manufactured [35] using the usual melt-quenching process for glass. However, due to their smaller phonon energy and greater rare-earth ion absorption, tellurite and germanate glasses [35] are excellent matrix materials for 2.7 µm.

When compared to other oxide glasses, germanate glass has the benefits of low phonon energy and robust infrared transmission across a vast wavelength range. Also, the presence of high viscosity and a significant number of hydroxyl groups may result in a strong absorption band of about 2.7 µm, which is detrimental to the emission of mid-infrared light. It is then necessary to modify germanate glass by replacing elements with La_2O_3 and Y_2O_3. Further elements, such as La_2O_3 and Y_2O_3, may be added to or substituted for the germanate glass. Because of its capacity to collect non-bridging oxygen from glass, the addition of La_2O_3 is predicted to increase glass forming ability. The addition of Y_2O_3, on the other hand, is expected to enhance thermal conductivity and considerably decrease the OH concentration in glass. The spectroscopic characteristics and mid-infrared emissions of La_2O_3 and Y_2O_3-modified germanate glass were studied by Jewell et al. [20]. As a further point of reference, Muzhi Cai et al. [50] explore relevant research from a new scientific method perspective because Jewell first researched it in the twentieth century. His publication studied thermal stability and spectroscopic characteristics for the GeO_2-Ga_2O_3-BaO-R_2O_3-5NaF-Er_2O_3 system (R = La, Y).

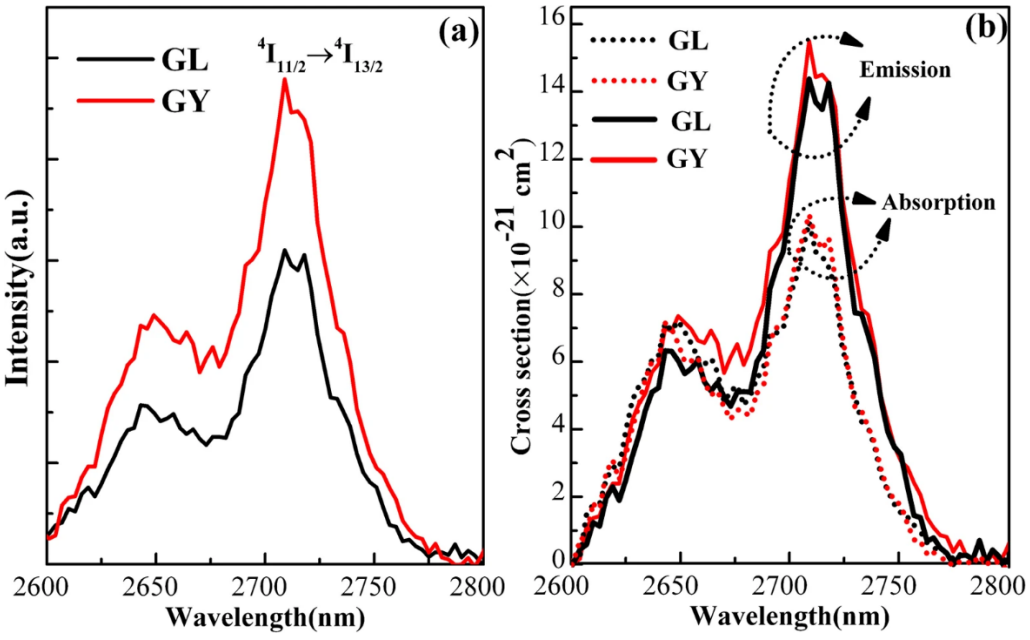

Figure 16: The prepared samples' fluorescence spectra at 2.7um (a) and the cross sections (emission and absorption) of the prepared samples (b) [50]

An 808 nm LD is used to excite Er^{3+} doped GL and GY glasses into the mid-infrared region, as shown in Figure 15. (LD). The 2.7 μm emissions of each of these glasses may be seen in Fig. 14a. The 2.7 μm emission intensity of GY glass is higher than that of GL glass. Research performed by Muzhi Cai [50] shows that the Y_2O_3 transformed germanate glass has superior spectroscopic characteristics than the La_2O_3 modified germanate glass, making it a good choice for mid-infrared optical particles.

4.2 Crystals in glass

Even in daily life, glass-ceramics are used in various applications, including cookware, electric stovetops, building materials, telescope mirrors, liquid crystal displays, solar cells, and photonic devices [40]. Due to the big interest in this material, researchers have focused their efforts on characterizing the crystallization mechanisms of numerous glass systems, including silicate [4, 5], tellurite [6], and chalcogenide glasses [7].

An investigation into RE-doped phosphate glass-ceramics has been conducted owing to the potential of increasing the luminescence of the RE ions by surrounding them with a crystalline environment [21–19]. The Er^{3+} ions may precipitate within the crystals of Er^{3+} doped phosphate GCs after they have been subjected to post-heat treatment, which may enhance the optical characteristics of the materials.

Based on the findings of Yu et al. [15, 18], compared to as-prepared glasses with the comparable composition, the intensity of the emission at X nm of Er^{3+} / Yb^{3+} co-doped phosphate glass-ceramics increased by a factor of 2. The 2.7 μm emission properties of glass-ceramics (GCs) are studied in the paper by Wei et al. [30]

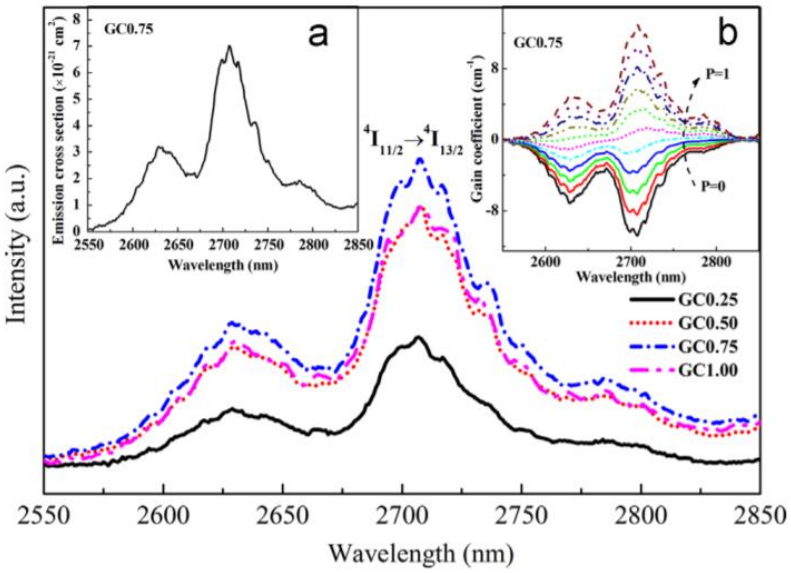

Figure 4: Mid-infrared fluorescence spectra of samples pumped at 980 nm[30]

Fig. 17 illustrates the mid-infrared emission spectra of glass-ceramics containing Er^{3+}: $NaYF_4$ nanocrystals. The intensity of the 2.7 m emission rises with the Er^{3+} concentration. With an

Er^{3+} concentration of 1.00 mol percent, the emission intensity at 2.7 μm reduces marginally, which may be attributed to the concentration quenching effect when the ideal doping percentage of Er^{3+} in produced glass-ceramics is 0.75 mol percent. Under 980 nm LD illumination, a strong 2.7 μm emission generated from the Er^{3+} : $^4I_{11/2} \rightarrow {}^4I_{13/2}$ transition was produced due to the integration of Er^{3+} ions into the precipitated $NaYF_4$ nanocrystals. As a result, we could assume that Er^{3+} doped oxyfluoride aluminosilicate glass-ceramic containing $NaYF_4$ may give a unique approach for mid-infrared purposes [29].

4.3 Addition of dopants

First and foremost, in 2021, Yu Zhang et al. investigated 2.7 μm emission in Er^{3+} co-doped tellurite glass. Ho^{3+} was added to Er^{3+} doped tellurite glass in his study to increase the 2.7 μm emission. By measuring visible, near and mid-infrared spectrum fluorescence emissions, the enhanced impact of Ho^{3+} on 2.7 μm emission induced by the 808 nm LD excitation was demonstrated. The conventional melt-quenching procedure was used to manufacture Er^{3+} single-doped and Er^{3+}/Ho^{3+} co-doped tellurite glasses with a composition of $75TeO_2$-(14.5-x)ZnO-$5ZnF_2$-$5Na_2O$ -0.5 Er_2O_3-xHo_2O_3 in mol percent, where x = 0, 0.3, 0.5, and 0.8 mol percent, and were designated as 0.5Er, 0.5Er0.3Ho, 0.5Er0.5Ho and 0.5Er0.8Ho respectively [39]

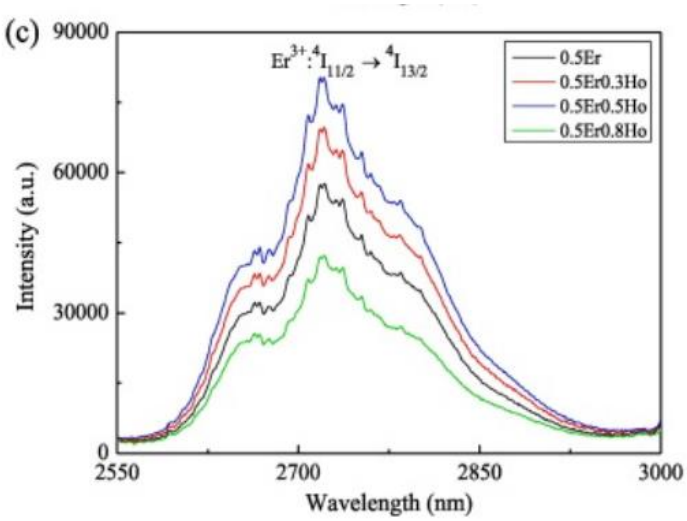

Figure 18: Photoluminescence spectra in the range of 2550-3000nm of Er^{3+} single-doped and Er^{3+}/Ho^{3+}co-doped tellurite glasses under the excitation of 808 nm.

Fig. 18 shows the luminescence spectra of Er^{3+} single-doped and Er^{3+}/Ho^{3+} co-doped tellurite glasses at 2.7 μm. Furthermore, it's seen that the amplitude of this mid-infrared band emission varies significantly when Ho^{3+} ions are added, demonstrating the efficiency of inserting Ho^{3+} ions in increasing the mid-infrared emission. The finding indicates that Ho^{3+} may intensify 2.7 μm emission. Because of these findings, co-doped tellurite glass with Er^{3+} and Ho^{3+} might be an attractive substrate for the construction of fiber amplifiers and lasers [47].

Continuously, Xiaomeng et al. [35] demonstrated that silver (Ag) nanoparticles had a substantial effect on the luminescence intensity of rare-earth ion-doped glass when measured under a 2.7 μm emission spectrum. It was possible to record the MIR emission spectra of Er^{3+} Ag co-doped BGN samples stimulated under 980 nm LD and display them in Figure 19. The

2.7 μm intensity emission increases as the amount of AgCl in the samples increases. Glass with 1.5 mol percent AgCl fluorescence intensity of Er^{3+} was designed to attain its maximum value and be 1.6 times greater than glass without AgCl throughout the research. After reading a study publication, he came to the conclusion that he had developed nanocomposites that are potential candidate host matrices for lasers[38], optical displays[38], and optical memory devices[38], among other things.

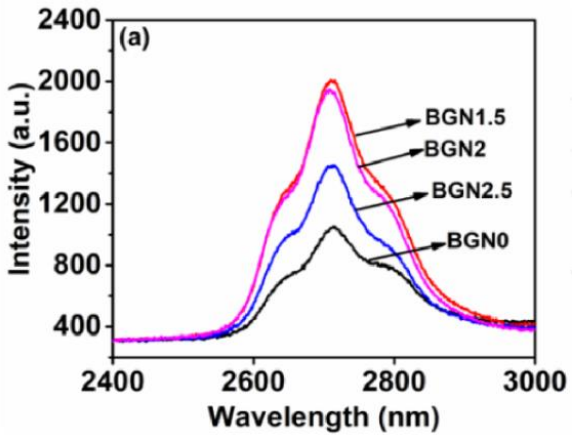

Figure 19: Fluorescence spectra of BGN2 samples. The spectra were acquired under excitation at (a) 2.7 μm;

5. CONCLUSIONS

In recent decades, MIR lasers operating at roughly three microns have sparked growing interest, with most of the attention being concentrated on achieving a 2.7 μm emission coherent MIR light source due to the several lucrative uses it has to offer. A literature review on obtaining a high-efficiency mid-infrared lasing output matching to the $^4\mathrm{I}_{11/2} \rightarrow {}^4\mathrm{I}_{13/2}$ transition at 2.7 μm emissions was the goal of this study.

After describing glass production methods such as sol-gel chemistry, and melt-quenching process, film deposition and fiber drawing as well as glass theory, a chapter was focused on the various solutions developed to improve the spectroscopic properties of the materials, including a modification in the glass system, the creation of glass-ceramics, and the use of a direct doping approach.

Various solutions were discovered, including a modification in the glass system, the creation of glass-ceramics, and the use of a direct doping approach. For much of this study, we will be talking about amplification of mid-infrared emission, which occurs at around 2.7 μm in wavelength and has been seen by many distinct ions in a number of different studies. In the next section, research publications on how to improve 2.7μm mid-infrared emission in Er^{3+} by using co-doped glass material are reviewed. We concentrated our efforts mostly on germanate glassed doping using a variety of ions. Under 808 nm excitation, it was discovered that Er^{3+}/Nd^{3+} co-doped germanate glass emits a more intense 2.7 μm emission. Because both samples were prepared and measured under the same experimental conditions, it is possible to conclude that the increased 2.7 μm emission is due to the increased absorption of pump energy, the increased energy transfers (ETs) of Er3+ ions, and the shorter lifetime of the lower lasing level Er^{3+} : $^4\mathrm{I}_{13/2}$ state when co-doping with Nd3+ ions when co-doping with Nd^{3+} ions Because of the exhibited findings, it seems that Er^{3+}/Nd^{3+} co-doped germanate glass has the potential to be employed as an efficient gain medium in the 2.7 μm glass fiber laser system under consideration.

Curiously, there are a few difficult challenges to address as well as practical suggestions for continuing this research to obtain a better result. Future efforts should be focused on continuing the development of glass-ceramics and more importantly on the direct doping method for the fabrication of new composites. New techniques to reduce the amount of OH to maximize the intensity of the MIR emission should also be investigated

REFERENCES

[1] P. W. MCMILLAN, Glass-Ceramics. 2nd edition. “Non-Metallic Solids”, edited by J. P. Roberts. Vol. 1, (London: Academic Press Inc. (London) Ltd. 1979).

[2] Schawlow, A. L., & Townes, C. H. (1958). Infrared and Optical Masers. The Physical Review, 112(6), 1940–1949. doi:10.1103/physrev.112.1940

[3] Maiman, T. H. (1960). Stimulated optical radiation in Ruby. Nature, 187(4736), 493–494. doi:10.1038/187493a0

[4] The 50 best innovation of 2011. Time Mag. Available: http://www.time.com/time/ magazine/article/0,9171,2099708,00.html

[5] Willner, A. E., Byer, R. L., Chang-Hasnain, C. J., Forrest, S. R., Kressel, H., Kogelnik, H., Tearney, G. J., Townes, C. H., & Zervas, M. N. (2012). Optics and Photonics: Key Enabling Technologies. Proceedings of the IEEE, 100(Special Centennial Issue), 1604–1643. https://doi.org/10.1109/jproc.2012.2190174 .

[6] Tsang, Y. H., El-Taher, A. E., King, T. A., & Jackson, S. D. (2006). Efficient 2.96 μm dysprosium-doped fluoride fibre laser pumped with a Nd:YAG laser operating at 1.3 μm. Optics Express, 14(2), 678. doi:10.1364/opex.14.000678

[7] Opt. Express 14, 678–685 (2006).

[8] Zhou, P., Wang, X., Ma, Y., Lü, H., & Liu, Z. (2012). Review on recent progress on mid-infrared fiber lasers. *Laser Physics*, *22*(11), 1744–1751. https://doi.org/10.1134/s1054660x12110199

[9] Fan, J., Yuan, X., Li, R., Dong, H., Wang, J., & Zhang, L. (2011). Intense photoluminescence at 27 μm in transparent Er^3+:CaF_2-fluorophosphate glass microcomposite. *Optics Letters*, *36*(22), 4347. https://doi.org/10.1364/ol.36.004347

[10] Wang, L., & Mizaikoff, B. (2008). Application of multivariate data-analysis techniques to biomedical diagnostics based on mid-infrared spectroscopy. *Analytical and Bioanalytical Chemistry*, *391*(5), 1641–1654. https://doi.org/10.1007/s00216-008-1989-9.

[11] Yao, Y., Hoffman, A. J., & Gmachl, C. F. (2012). Mid-infrared quantum cascade lasers. *Nature Photonics*, *6*(7), 432–439. https://doi.org/10.1038/nphoton.2012.143

[12] Zachariasen, W. H. (1932). THE ATOMIC ARRANGEMENT IN GLASS. *Journal of the American Chemical Society*, *54*(10), 3841–3851. https://doi.org/10.1021/ja01349a006

[13] Shelby, J. E. (2005). Introduction to Glass Science and Technology. 2nd. Cambridge: The Royal Sosiety of Chemistry.

[14] Paradisi, A., Biscaras, J., & Shukla, A. (2015). Space charge induced electrostatic doping of two-dimensional materials: Graphene as a case study. *Applied Physics Letters*, *107*(14), 143103. https://doi.org/10.1063/1.4932572

[15] Fan, J., Yuan, X., Li, R., Dong, H., Wang, J., & Zhang, L. (2011b). Intense photoluminescence at 27 μm in transparent Er^3+:CaF_2-fluorophosphate glass microcomposite. *Optics Letters*, *36*(22), 4347. https://doi.org/10.1364/ol.36.004347

[16] R. Reisfeld and C. K. Jùrgensen, Excited State Phenomena in Vitreous Materials, Handbook on the Physics and Chemistry of Rare Earth 9, ed. K. A. Gschneidner Jr. and L. Eyring, 1987

[17] Harsha, P. K. S. S. (2005). Principles of Vapor Deposition of Thin Films. Elsevier Gezondheidszorg, 1160 p.

[18] Xu, B., Hao, J., Guo, Q., Wang, J., Bai, G., Fei, B., Zhou, S., & Qiu, J. (2014). Ultrabroadband near-infrared luminescence and efficient energy transfer in Bi and Bi/Ho co-doped thin films. *Journal of Materials Chemistry C*, *2*(14), 2482. https://doi.org/10.1039/c3tc32177k

[19] McClanahan, E. D. (1991). Production of thin films by controlled deposition of sputtered materia. SpringerLink. https://link.springer.com/chapter/10.1007/3540534288_21?error=cookies_not_supported&code=f2d45cb0-d99f-4ca1-bb56-0c9d8f986abf

[20] Shelby, J. E. (2005). Introduction to Glass Science and Technology (Rsc Paperbacks) (2nd ed.). Royal Society of Chemistry.

[21] Kassab, L. R., Silva, D. M., Garcia, J. A., da Silva, D. S., & de Araújo, C. B. (2016). Silver nanoparticles enhanced photoluminescence of Nd 3+ doped germanate glasses at 1064 nm. *Optical Materials*, *60*, 25–29. https://doi.org/10.1016/j.optmat.2016.07.006

[22] C. Gonçalves, L. Santos, R. Almeida, Rare-earth-doped transparent glass-ceramics, Comptes Rendus Chimie Vol. 5, 2002, pp. 845–854

[23] Guojun Gao, Guonian Wang, Chunlei Yu, Junjie Zhang, Lili Hu, Investigation of 2.0μm emission in Tm3+ and Ho3+ co-doped oxyfluoride tellurite glass,Journal of Luminescence, Volume 129, Issue 9,2009, Pages 1042-1047, ISSN 0022-2313, https://doi.org/10.1016/j.jlumin.2009.04.024

[24] Enhanced 2.7 μm emission and energy transfer mechanism of Nd3+/Er3+ co-doped sodium tellurite glasses. (2011). Journal of Applied Physics, 110(1), 013512. https://doi.org/10.1063/1.3601353

[25] Tian, Y., Xu, R., Hu, L., & Zhang, J. (2012). 2.7μm fluorescence radiative dynamics and energy transfer between Er3+ and Tm3+ ions in fluoride glass under 800nm and 980nm excitation. Journal of Quantitative Spectroscopy and Radiative Transfer, 113(1), 87–95.

[26] Tian, Y., Xu, R., Hu, L., & Zhang, J. (2011). Spectroscopic properties and energy transfer process in Er3+ doped ZrF4-based fluoride glass for 2.7μm laser materials. Optical Materials, 34(1), 308–312. https://doi.org/10.1016/j.optmat.2011.09.004

[27] Huang, F., Li, X., Liu, X., Zhang, J., Hu, L., & Chen, D. (2014). Sensitizing effect of Ho3+ on the Er3+: 2.7μm-emission in fluoride glass. Optical Materials, 36(5), 921–925. https://doi.org/10.1016/j.optmat.2013.12.031

[28] Faucher, D., Bernier, M., Caron, N., & Vallée, R. (2009). Erbium-doped all-fiber laser at 294 μm. Optics Letters, 34(21), 3313. https://doi.org/10.1364/ol.34.003313

[29] Zhao, J., Zheng, X., Schartner, E. P., Ionescu, P., Zhang, R., Nguyen, T., Jin, D., & Ebendorff-Heidepriem, H. (2016). Upconversion Nanocrystal-Doped Glass: A New Paradigm for Photonic Materials. Advanced Optical Materials, 4(10), 1507–1517. https://doi.org/10.1002/adom.201600296

[30] Jewell, J. M., Higby, P. L., & Aggarwal, I. D. (1994). Properties of BaO-R2O3- Ga2O3-GeO2 (R = Y, Al, La, and Gd) Glasses. Journal of the American Ceramic Society, 77(3), 697–700. https://doi.org/10.1111/j.1151-2916.1994.tb05351.x

[31] Wei, T., Tian, Y., Tian, C., Jing, X., Li, B., Zhang, J., & Xu, S. (2016). 2.7 μm emissions in Er 3+ : NaYF 4 embedded aluminosilicate glass ceramics. Ceramics International, 42(1), 1332–1338. https://doi.org/10.1016/j.ceramint.2015.09.071

[32] Suyver, J., Grimm, J., van Veen, M., Biner, D., Krämer, K., & Güdel, H. (2006). Upconversion spectroscopy and properties of NaYF4 doped with , and/or. Journal of Luminescence, 117(1), 1–12. https://doi.org/10.1016/j.jlumin.2005.03.011

[33] Nguyen, H., Tuomisto, M., Oksa, J., Salminen, T., Lastusaari, M., & Petit, L. (2017). Upconversion in low rare-earth concentrated phosphate glasses using direct NaYF 4 :Er 3+ , Yb 3+ nanoparticles doping. Scripta Materialia, 139, 130–133. https://doi.org/10.1016/j.scriptamat.2017.06.050

[34] F. Gan, L. Xu, Photonic Glasses, World Scientific Pubishing Co. Pte. Ltd (2006) 447

[35] M. P. Hehlen, M. L. F Philips, N. J. Cockroft, H. U. Güdel, Encyclopedia of Materials: Science and Technology, Burschow, K. H. J., Ed.; Elsevier Science Ltd.: New York 10 (2001) 9456.

[36] Jia, X., Xia, M., Xu, Y., Yang, L., Zhang, Y., Li, M., & Dai, S. (2018). Silver nanoparticle enhanced 27 μm luminescence in Er3+-doped bismuth germanate glasses. Optical Materials Express, 8(6), 1625. https://doi.org/10.1364/ome.8.001625

[37] Wu, Y., Shen, X., Dai, S., Xu, Y., Chen, F., Lin, C., Xu, T., & Nie, Q. (2011). Silver Nanoparticles Enhanced Upconversion Luminescence in Er3+/Yb3+ Codoped Bismuth-Germanate Glasses. The Journal of Physical Chemistry C, 115(50), 25040–25045. https://doi.org/10.1021/jp207035c

[38] Jiang, Y., Fan, J., Jiang, B., Mao, X., Tang, J., Xu, Y., Dai, S., & Zhang, L. (2016). Er3+-doped transparent glass ceramics containing micron-sized SrF2 crystals for 2.7 μm emissions. Scientific Reports, 6(1). https://doi.org/10.1038/srep29873

[39] E.D. McClanahan, N. Laegreid, Production of thin films by controlled deposition of sputtered material. In: Behrisch R., Wittmaack K. (eds) Sputtering by Particle Bombardment III. Topics in Applied Physics, Vol. 64, 1991

[40] Wen, S., Wang, Y., Lan, B., Zhang, W., Shi, Z., Lv, S., Zhao, Y., Qiu, J., & Zhou, S. (2019). Pressureless Crystallization of Glass for Transparent Nanoceramics. Advanced Science, 6(17), 1901096. https://doi.org/10.1002/advs.201901096

[41] Shelby, J. E. (2005). Introduction to Glass Science and Technology. 2nd. Cambridge: The Royal Sosiety of Chemistry, 291 p

[42] Mortier, M. (2002). Between glass and crystal: Glass–ceramics, a new way for optical materials. Philosophical Magazine B, 82(6), 745–753. https://doi.org/10.1080/13642810208224364

[43] MClara Gonçalves, M., Santos, L. F., & Almeida, R. M. (2002). Rare-earth-doped transparent glass ceramics. Comptes Rendus Chimie, 5(12), 845–854. https://doi.org/10.1016/s1631-0748(02)01457-1

[44] M. Yamane, Y. Asahara, Glasses for Photonics, Cambridge University Press, Cambridge, 2000, 284 p.

[45] Dantelle, G., Mortier, M., Vivien, D., & Patriarche, G. (2006). Influence of Ce3+ doping on the structure and luminescence of Er3+-doped transparent glass-ceramics. Optical Materials, 28(6–7), 638–642. https://doi.org/10.1016/j.optmat.2005.09.008

[46] Liu, G., Jacquier, B., &) B. J. (2005). Spectroscopic Properties of Rare Earths in Optical Materials. Springer Publishing.

[47] Zhao, J.; Zheng, X.; Schartner, E. P.; Ionescu, P.; Zhang, R.; Nguyen, T. L.; Jin, D.; Ebendorff-Heidepriem, H. Upconversion Nanocrystal-Doped Glass: A New Paradigm for Photonic Materials. Adv. Opt. Mater. 2016, 4, 1507–1517, doi:10.1002/adom.201600296.

[48] Zhang, Y., Xia, L., Li, C., Ding, J., Li, J., & Zhou, Y. (2021). Enhanced 2.7 μm mid-infrared emission in Er3+/Ho3+ co-doped tellurite glass. Optics & Laser Technology, 138, 106913. https://doi.org/10.1016/j.optlastec.2021.106913

[49] Popa, D., & Udrea, F. (2019). Towards Integrated Mid-Infrared Gas Sensors. Sensors, 19(9), 2076. https://doi.org/10.3390/s19092076.

[50] Hishimone, P. N., Nagai, H., & Sato, M. (2020, July 8). Methods of fabricating thin films for Energy Materials and Devices. IntechOpen. Retrieved December 14, 2021,

[51] Cai, M., Zhou, B., Wang, F., Wei, T., Tian, Y., Zhou, J., Xu, S., & Zhang, J. (2015).

R2O3 (R = La, Y) modified erbium activated germanate glasses for mid-infrared 2.7 μm laser materials. Scientific Reports, 5(1). https://doi.org/10.1038/srep13056

[52] Faraji, G., Kim, H. S., & Kashi, H. T. (2018). Severe Plastic Deformation. Elsevier Gezondheidszorg. (pp. 1–17). Elsevier.

[53] Peter W. Werle, Karl Maurer, Robert Kormann, Franz Slemr, Robert Josef Muecke, and Bernd Jaenker(23 September 2002); "Near- and mid-infrared laser sensors for atmospheric gas analysis", Proc. SPIE 4817, Diode Lasers and Applications in Atmospheric Sensing, https://doi.org/10.1117/12.451422

[54] Image courtesy of Spectrogon. NB-2710-050 nm Ø25.4x1.0 mm. Available: https://www.spectrogon.com/wp-content/uploads/spectrogon/NB-4270-085-nm.pdf

[55] Grdadolnik, Jože. "ATR-FTIR SPECTROSCOPY: ITS ADVANTAGES and LIMITATIONS." *National Institute of Chemistry*, 2002, www.researchgate.net/profile/Joze-Grdadolnik/publication/282592714_ATRFTIR_spectroscopy_Its_advantages_and_limitations/links/584bce7208aeb989251f1ae9/ATR-FTIR-spectroscopy-Its-advantages-and-limitations.pdf

[56] Joubert, Marie-France. "Photon Avalanche Upconversion in Rare Earth Laser Materials." *Elsevier, ScienceDirect*, Jan. 1999, reader.elsevier.com/reader/sd/pii/S0925346798000433?token=8EE8F1924149585E9DC06336DF6D949BFAFD2739AD8F015DA477A483B243FCF200E6F9CB12F32788F48BEF0B7D489F69&originRegion=eu-west-1&originCreation=20220406225936. Accessed 6 Apr. 2022.

[57] Zhao, Xinyu, et al. "Design of Infrared-Emitting Rare Earth Doped Nanoparticles and Nanostructured Composites." *Journal of Materials Chemistry C*, vol. 4, no. 36, 2016, pp. 8349–8372, 10.1039/c6tc02373h. Accessed 6 Apr. 2022.

[58]